Science of the Total Environment 980 (2025) 179545

Contents lists available at ScienceDirect

Science of the Total Environment

journal homepage: www.elsevier.com/locate/scitotenv

Nanoplastic exposure affects the intestinal microbiota of adult *Drosophila* flies

Arnau Rocabert [a], Joan Martín-Pérez [a], Laia Pareras [a], Raquel Egea [a], Mohamed Alaraby [a], Jordi Manuel Cabrera-Gumbau [b], Iris Sarmiento [b], Jaime Martínez-Urtaza [b], Laura Rubio [a], Irene Barguilla [a], Ricard Marcos [a], Alba García-Rodríguez [a,*], Alba Hernández [a,*]

[a] Group of Mutagenesis, Department of Genetics and Microbiology, Faculty of Biosciences, Universitat Autònoma de Barcelona, Cerdanyola del Vallès, Spain
[b] Group of Genomics, Bioinformatics & Evolutionary Biology, Department of Genetics and Microbiology, Faculty of Biosciences, Universitat Autònoma de Barcelona, Cerdanyola del Vallès, Spain

HIGHLIGHTS

- *Drosophila* was used to determine intestinal dysbiosis induction by nanoplastics.
- PS (a petroleum-based polymer) and PLA (a bio-based polymer) NPLs were used.
- No previous studies on dysbiosis induced by MNPLs in *Drosophila* were found.
- Both MNPL types reduce diversity and richness of the *Drosophila* gut microbiome.
- PSNPLs effects were more marked than those induced by PLA.

GRAPHICAL ABSTRACT

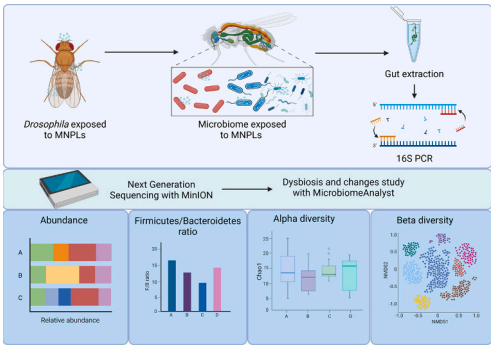

ARTICLE INFO

Editor: Ouyang Wei

Keywords:
Drosophila melanogaster
MNPLs
PCR
16S sequencing
MinION
Nanopore
Microbiota
Dysbiosis

ABSTRACT

Micro- and nanoplastics (MNPLs) are emerging environmental pollutants that have garnered significant attention over the past few decades due to their detrimental effects on human health through various exposure pathways. This study investigates the impact of MNPLs on gut microbiota, utilizing *Drosophila melanogaster* as a model organism. *Drosophila* was selected for its microbiota's similarities to humans and its established role as an accessible and well-characterized model system. To analyze microbiota, full-length 16S rRNA gene sequencing was performed using the Nanopore sequencing platform, enabling comprehensive profiling of the microbial populations present in the samples. As models of MNPLs, two commercial polystyrene nanoplastics (PS-NPLs, 61.20 and 415.22 nm) and one lab-made polylactic acid nanoplastic (PLA-NPLs, 463.90 nm) were selected. As a positive control, zinc oxide nanoparticles (ZnO-NPs) were used. The observed findings revealed that exposure to MNPLs induced notable alterations in gut microbiota, including a reduction in bacterial abundance and shifts in species composition. These results suggest that MNPLs exposure can lead to microbial dysbiosis and potential gut

* Corresponding authors at: Group of Mutagenesis, Department of Genetics and Microbiology, Faculty of Biosciences, Universitat Autònoma de Barcelona, Campus of Bellaterra, 08193 Cerdanyola del Vallès, Barcelona, Spain.
E-mail addresses: alba.garcia.rodriguez@uab.cat (A. García-Rodríguez), alba.hernandez@uab.cat (A. Hernández).

https://doi.org/10.1016/j.scitotenv.2025.179545
Received 13 February 2025; Received in revised form 27 March 2025; Accepted 24 April 2025
Available online 30 April 2025

health disruptions through its interaction, either with the gut epithelial barrier or directly with the resident microorganisms.

1. Introduction

The term “microbiota” can be defined as the community of microorganisms, encompassing bacteria, archaea, some unicellular eukaryotes, and viruses, that inhabit a specific environment (D’Argenio and Salvatore, 2015). In humans, the five primary sites housing microbiota are the gut, lungs, vagina, oral cavity, and skin, with the human gastrointestinal tract harbouring the most abundant microbial niche in the body. Although there are big differences between the reported number of microbiota cells, and its ratio with the total number of human cells, it is considered that the number of bacteria in the body is of the same order as the number of human cells, and their total mass is about 0.2 kg (Sender et al., 2016). Microbiota has co-evolved with the species throughout its existence. Thus, humans have developed over time an immune system capable of tolerating the presence of certain microorganisms at specific concentrations, while also defending against and eliminating invasive or undesirable pathogens (Dominguez-Bello et al., 2019). It is well known that alterations in the microbiota constitution can result in disruptions to human health, ranging from mild conditions like stomach aches to more severe diseases such as sclerosis, metabolic disorders, and neurological conditions, including type 2 diabetes, obesity, depression, and autism (Gomaa, 2020). Disruptions in the balance of these microorganisms are referred to as "dysbiosis" of the human microbiota, and the key characteristics of dysbiosis include a loss of beneficial microorganisms, an increase in harmful ones, or a reduction in microbial diversity. In most of the cases, dysbiosis can be related to environmental exposure (Campana et al., 2022). Thus, discovering environmental pollutants potentially related to dysbiosis is required.

A growing body of scientific evidence shows the harmful effects of micro/nanoplastics (MNPLs) on human health as environmental pollutants. Recent studies have highlighted that plastic pollution may also be impacting microbiome communities, due to the accumulation of plastics in various habitats such as oceans, rivers, and forests. This issue is particularly concerning in aquatic environments, where the buildup of plastics has become a significant problem. A recent review shows the high presence of MNPLs in edible seafood pointing out the associated risk and the relevance to safeguard food safety and human health (Woh et al., 2024). When MNPLs are ingested by the organisms the intestine is the first target, frequently causing increased intestinal permeability and decreased immune response associated with inflammation (Niu et al., 2023). Once MNPLs cross the intestinal barrier they tend to accumulate primarily in the liver, kidneys, and gastrointestinal tract. Prolonged interaction between MNPLs and these organs can result in histopathological changes, leading to tissue damage and dysfunction. When reviewing the potential effects of MNPLs in microbiota, zebrafish and mice are the most used animal models. Such studies demonstrate the potential of MNPLs to triggers intestinal dysbiosis, causing the enrichment of harmful bacteria (Firmicutes, Proteobacteria, and Chlamydia) and a reduction of beneficial organisms such as Bacteroidetes phylum abundance (Souza-Silva et al., 2022).

Drosophila melanogaster is a widely used model organism in scientific research due to its many advantageous properties, these include the low cost of maintenance, their rapid growth rate and high number of offspring, which allow for inexpensive and rapid genetic studies; their genetic similarity to mammals also allows for studies done in *Drosophila* to be extrapolated to humans and lastly, the knowledge of the whole genome, as well as the use of different genetic tools, allows the study of gene function and disease mechanisms (Wāng and Jiang, 2024). Such model has been useful to detect the potential health effects of MNPL exposure including their fate, tissue interactions, and effects on the intestinal barrier (Drosophila’s midgut) and resident gut bacteria (Alaraby et al., 2022, 2023). No studies have been found in literature detecting the potential ability of MNPLs to disrupt *Drosophila* microbiota. Nevertheless, various studies have utilized both *Drosophila* larvae and adult flies to investigate the effects of different environmental toxicants like stilbenoids, sulfamethoxazole, lead, and microplastics, among others, and the influence of microbiota across developmental stages. Thus, when lead effects in both gut microbiota and neurotoxicity targets were evaluated, alpha and beta diversity of gut microbiota were significantly different between the flies exposed to lead acetate (at 200 μg/mL) and the controls. Two genera, *Lactobacillus* and *Bifidobacterium* were found significantly decreased in the exposed flies and these effects significantly correlated with the learning and memory decreases (Sun et al., 2020). In addition, exposure to lead reduced viability in *D. melanogaster* decreasing *Lactobacillus* abundance and increasing the presence of *Wolbachia*. Alternatively, in the species *D. subobscura,* exposure caused shifts in developmental time but maintained the egg-to-adult viability at a similar level. Regarding microbiota diversity results indicated that *Komagataeibacter* could be a valuable member of *D. subobscura* microbiota in overcoming the environmental stress (Beribaka et al., 2021). Sodium benzoate exposure effects on microbiota have also been evaluated showing that exposure affects host growth and development of *Drosophila* through altering endocrine hormone levels and commensal microbial composition (Dong et al., 2022). Hence, due to the previously indicated advantages above mentioned, *D. melanogaster* is a valuable model for investigating the genetic and environmental factors influencing intestinal microbiota dynamics and host-microbiome interaction.

To better understand which type of interaction exists between ingested MNPLs and gut microbiota, changes in their composition were determined by 16S rRNA microbial community profiling in exposed adult *Drosophila* flies. To determine if differences in the MNPL characteristics modulate the induced effects, commercial polystyrene nanoplastics (PS-NPLs) and real-life polylactic acid nanoplastics (PLA-NPLs) obtained from the degradation of plastic pellets were used. Additionally, ZnO-NPs, a well-known antimicrobial particulate agent, was used as positive control.

2. Materials and methods

2.1. Nanoplastic obtention, preparation and characterization

The two types of PS-NPLs used in this study were obtained from Spherotech (Lake Forest, IL, USA). Specifically, they are named as PS50 (80 nm; reference SPH-PP-008-10) and PS500 (430 nm; reference SPH-PP-05-10). On the other hand, polylactic acid (PLA) nanoplastics were prepared as previously described (Alaraby et al., 2024a). Briefly, the used method involves dissolving the polymer in a solvent and then evaporating the solvent to reach the desired particle size and characteristics. The positive control, ZnO-NPs (NM110) was supplied by the NANoREG consortium, and the EU Joint Research Centre at Ispra (Italy). To disperse the selected NPLs, they were pre-wetted with 0.5 % absolute ethanol and subsequently suspended in 0.05 % filtered bovine serum albumin (BSA) prepared in autoclaved Milli-Q water. The suspension was sonicated for 16 min at 10 % amplitude, yielding a well-dispersed stock solution with a final concentration of 2.56 mg/mL, following the NanoGenotox protocol (NanoGenotox, 2011). The characterization of the NPLs used in this study, including their shape, morphology, surface charge, and aggregation status, was performed using scanning electron microscopy (SEM, Zeiss Merlin, Zeiss, Oberkochen, Germany), transmission electron microscopy (TEM, JEOL JEM 1400, JEOL LTD, Tokyo, Japan), and a Zetasizer Nano-ZS zen3600 instrument (Malvern Panalytical, Malvern, UK).

2.2. Drosophila strain and exposure conditions

The Canton-S strain of *D. melanogaster* was used as model organism in this study. The flies were reared at 25 °C with a 12-h light/dark cycle in crystal flasks containing a medium composed of agar, salt, fresh yeast, corn, nipagin (diluted in ethanol as a preservative), and propionic acid for pH regulation. The flasks also included a piece of paper coated with antifungal agents to provide a resting place for the flies. All flies were transferred to a fresh medium weekly.

To expose adult *Drosophila* flies, the used NPLs were mixed with peach-grape juice, as follows. 1 mL of juice (only juice as negative control for unexposed flies, and NPLs diluted in juice for treated flies) was used to wet the bottom of the clean sponge plug, normally used as a stopper for flies' vials. In addition, a piece of paper was placed inside each vial to keep the flies' mobility-relax regime. Every two days, flies were transferred into new vials with new paper pieces and fresh wet plugs to reduce flies' mortality and keep a continuous feeding exposure lasting for one week (see Fig. 1). This exposure protocol has been recently published (Alaraby et al., 2024b). *Drosophila* flies were exposed to the same concentration for each NPL treatment, 100 μg/mL. This concentration was chosen to follow the same exposure regime as in previous studies where 100 μg/mL was found to be a sublethal concentration but suitable to track all the NPLs journey along the *Drosophila's* midgut (Alaraby et al., 2022, 2023, 2024a).

2.3. Drosophila gut extraction

Gut extraction was conducted *via* dissection. At day 7, just when exposure finished, adult flies were anaesthetised with ether and washed in ethanol for 30 s. To avoid contamination, the process was carried out in a sterile culture hood, using sterile tweezers and a sterile glass Petri-dish, the thorax was held in place while the abdomen was gently pulled apart, exposing the midgut, which remained connected to both body segments. The midgut was then extracted, collected in 1.5 mL Eppendorf tubes and freeze at –80 °C for further analysis. The guts of 50 flies were collected in triplicates for each treatment.

2.4. Visualisation of microorganisms by scanning electron microscopy (SEM) and transmission electron microscopy

Scanning electron microscopy (SEM) was used to visualise the presence of different microorganisms in the exposed individuals. To proceed, guts from 50 treated/non-treated flies were extracted, homogenized, filtered and covered with a fixative agent. In all cases 10–20 μL drops were deposited in a carbon-coated tab (Agar Scientific, Ltd., UK) and left to dry before imaging. Finally, several representative images were taken from a random field of view. Transmission electron microscopy (TEM) was used to visualise the presence of microorganisms in the lumen of the gut of the larvae. Following the protocol mentioned previously, 50 non-treated flies' guts were extracted and samples from the isolated intestines were processed to obtain ultrathin sections (100

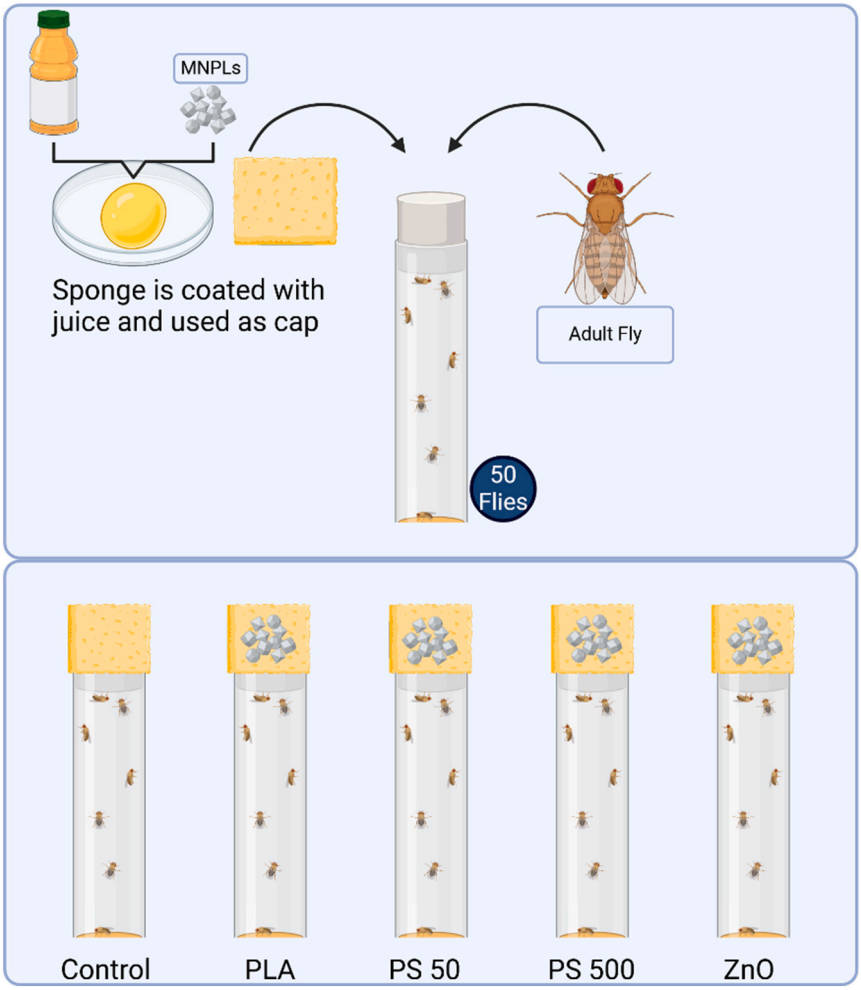

Fig. 1. Graphical representation of *Drosophila* feeding procedure. Flies feed inside tubes closed with juice-wetted sponge plug. Paper pieces were placed inside tubes to regulate fly activities. Triplicates were made for each treatment.

nm in thickness) that were placed on non-coated 200 mesh copper grids. The intestinal sections were contrasted with uranyl acetate and visualised by TEM (Jeol 1400,100 kV) equipped with a CCD Gatan ES1000w Erlangshen Camera (Gatan Inc., Pleasanton, CA, USA).

2.5. DNA extraction

To extract DNA from microorganism's guts, the ZymoBIOMICS™ DNA Miniprep Kit (Zymo Research Corporation, Orange, CA, USA) was utilized. This advanced microbial DNA purification kit is specifically designed for extracting DNA from various sample types, making it ideal for microbiome and metagenomic analyses. The ZymoBIOMICS lysis technology minimises bias caused by differential lysis efficiency among organisms, ensuring more accurate microbial community profiling. The extraction process involved homogenising the gut samples, which were then placed into a bead-beating tube containing ultra-high-density BashingBeads™. To achieve a rapid and thorough homogenization, samples were processed with filters and chemical methods. After cell lysis, inhibitor removal technology was applied to eliminate potential contaminants. The total genomic DNA was then captured on a silica membrane using a spin column, followed by a series of washes and elution steps to prepare DNA for downstream applications. All procedures were carried out according to the manufacturer's instructions. The quantity of isolated genomic DNA was measured using a fluorometric assay (Qubit 4 Fluorometer, Thermo Fisher Scientific) and stored at -20 °C until further use.

2.6. 16S amplification

The tailed primers used for the amplification of the full length of the 16S rRNA gene (including all the V1-V9 regions) were as follows (Johnson et al., 2019):

forward primer (27F):

5' TTTCTGTTGGTGCTGATATTGC-[AGAGTTTGATCMTGGCTCAG] 3'

and reverse primer (1492R):

5' ACTTGCCTGTCGCTCTATCTTC-[CGGTTACCTTGTTACGACTT] 3'

DNA amplification was carried out using a BIOER XP thermal cycler. The reaction mix contained 12.5 μL of LongAmp® Hot Start Taq 2× Master Mix (New England Biolabs), 0.4 μM of each primer, 15 ng of sample DNA, and Milli-Q water to a final volume of 25 μL. The thermocycling profile consisted of an initial denaturation at 95 °C for 3 min, followed by 5 cycles of amplification (95 °C for 15 s, 55 °C for 15 s, and 65 °C for 90 s). This was followed by 30 additional cycles (95 °C for 15 s, 62 °C for 15 s, and 65 °C for 90 s), and a final elongation at 65 °C for 2 min. In cases where DNA concentration was particularly low and did not meet the 15-ng requirement, a reaction mix with double the number of reagents and a final volume of 50 μL was used. After PCR, a purification step was necessary to remove excess reagents and prevent interference in subsequent reactions. This was performed using the AMPure XP bead system (Beckman Coulter, Inc.) according to the manufacturer's instructions. The system provides a fast and efficient cleanup process, allowing for size selection based on the number of beads used. If an insufficient number of beads is applied, smaller fragments may not bind and will be discarded. The volume ratio between beads and PCR products was 1:1. The concentration of the amplified DNA was measured using a fluorometric assay (Qubit 4 Fluorometer, Thermo Fisher Scientific) and stored at −20 °C until further use.

2.7. Barcoding PCR

The barcoding of DNA was performed using a PCR reaction with a mixture consisting of 25 μL of LongAmp® Taq 2× Master Mix (New England Biolabs), 154 fmol (150 μg) of the previously purified PCR product, 1 μL of the desired barcode for each sample from the EXP-PBC096 barcoding kit (Oxford Nanopore Technologies, ONT), and Milli-Q water to bring the total volume to 50 μL.

The PCR amplification followed this temperature profile: an initial denaturation at 95 °C for 3 min, followed by 15 cycles (95 °C for 15 s, 62 °C for 15 s, and 65 °C for 90 s), and a final elongation step at 65 °C for 2 min. After the amplification, the PCR products were purified using the AMPure XP bead system (Beckman Coulter, Inc.), with a bead-to-sample volume ratio of 1:1. The purified product was eluted in 20 μL of Milli-Q water.

All barcoded samples were then pooled into a library at a desired ratio to achieve a total of 3000 ng in 147 μL, which was mixed in a 1.5 mL Eppendorf tube. If the pooled volume exceeded the desired amount, an additional purification step was performed. The quantity of the barcoded DNA was measured using a Qubit 4 Fluorometer (Thermo Fisher Scientific) and stored at -20 °C overnight for further processing.

2.8. Reparation of DNA

The next step in the process involved DNA end repair, also referred to as EndPrep, which phosphorylates the 5' ends and adds tails to the 3' ends of the DNA fragments. This was carried out using a thermal cycler with the following conditions: 20 °C for 5 min, followed by 65 °C for 5 min. The reaction mix included 49 μL of the pooled DNA library, 1 μL of a DNA control sample, 7 μL of NEBNext Ultra II End Prep Reaction Buffer (New England Biolabs), and 3 μL of NEBNext Ultra II End Prep Enzyme Mix (New England Biolabs). After the EndPrep reaction, the DNA was purified using the AMPure XP bead system (Beckman Coulter, Inc.), with a bead-to-sample volume ratio of 1:1. The repaired DNA was eluted in 61 μL of Milli-Q water. The concentration of the repaired DNA was measured using a Qubit 4 Fluorometer (ThermoFisher Scientific), and the samples were stored at -20 °C overnight for further use.

2.9. Adaptor ligation

The final step before priming the MinION flow cell, where sequencing will occur, involved the adapter ligation of the DNA library. This was done by mixing 60 μL of the repaired DNA with reagents from the SQK-LSK114 Ligation Sequencing Kit (ONT). The reaction mixture contained 25 μL of Ligation Buffer, 5 μL of Adapter Mix H, and 10 μL of NEBNext Quick T4 DNA Ligase (New England Biolabs). The mixture was incubated at room temperature for 10 min. Following this, the sample was purified using the AMPure XP bead system (Beckman Coulter, Inc.), according to the protocol provided by ONT. The quantity of the barcoded DNA was measured using a Qubit 4 Fluorometer (ThermoFisher Scientific). The prepared DNA can be stored at 4 °C for short-term use or at -80 °C for long-term storage (over 3 months).

2.10. Loading the MinION flow cell

From the prepared library, 45 fmol of DNA were diluted in 12 μL of Milli-Q water for the priming of the MinION flow cell. The priming and washing of the flow cell followed the manufacturer's protocols provided by ONT.

Metagenomic sequencing was carried out using the ONT MinION platform, with flow cells onto which all samples were loaded simultaneously. The priming procedure involved unloading any residual buffers from the flow cell and refilling it with a loading buffer, along with the prepared DNA sample. The washing process included emptying the flow cell again and filling it with a storage buffer, provided that enough nanopores remained active. For these protocols, the Flow Cell Priming Kit (EXP-FLP004) and the Flow Cell Washing Kit (EXP-WSH004) from ONT were used.

2.11. Bioinformatic analysis

All 16S rRNA sequences were obtained by the Min-KNOW suite and base called with Guppy 3.0. (ONT). Reads were filtered by length

(between 1000 bp and 2000 bp) and quality (> Q10) using Chopper 0.7.0 (De Coster and Rademakers, 2023). Adapters and barcodes were trimmed with Porechop 0.2.4 (Wick et al., 2017). Taxonomic assignment at the genus and species level was carried out with Emu 3.4.4 (Curry et al., 2022), using a database consisting of a combination of rrnDB v5.6 and NCBI 16S RefSeq on a 95 % of identity threshold (Klappenbach et al., 2001; O'Leary et al., 2016). Afterwards, taxa with single read counts were removed. In addition, a low count filter was set to a minimum read count of 10. Finally, filtered data was normalised using total sum scaling (TSS). Plots and analysis of microbiome structure and diversity were made by MicrobiomeAnalyst (Dhariwal et al., 2017). The goodness of this entire protocol was checked using a mock community (ZymoBIOMICS Microbial Community Standard D6300) of known species composition and abundance as internal control. Results are shown in the Supplementary Material.

3. Results and discussion

3.1. NPLs characterization

The NPLs used to expose adult *Drosophila* flies were first characterized, after dispersing them, using the previously indicated NanoGenotox protocol. Fig. 2 shows that all three NPLs present a perfect spherical shape, while ZnO-NPs show a more oval- or cylindrical-shaped forms. The average diameters for PS50, PS500, PLA-NPLs, and ZnO-NPs were 61.20, 415.22, 463.90, and 132.37 nm, respectively, when evaluated in their dry state. When dispersed, their hydrodynamic size (PS50: 73.74 nm, PS500: 488.90 nm, PLA-NPLs: 425.70 nm, and ZnO-NPs: 114.70 nm) did not differ substantially from its dry state, meaning little to non-aggregation. All the polydispersity indices were found significantly lower than 0.50, which describes the tendence off all particulate suspensions to be monodisperse. However, PS suspensions were the more monodispersed, followed by ZnO-NPs and PLAN-NPLs, respectively. The zeta-potential values indicate that all nanoparticles were positively charged on their surfaces but once again the PS suspensions were more stable than the PLA-NPLs and ZnO-NPs, since the values near ±30 mV would suggest that particles are repealing each other strongly, preventing aggregation. PLA-NPL and ZnO-NP suspensions, however, presented a moderate stability (values between ±10 to ±30 mV), where some aggregation may occur depending on external factors like pH, ionic strength, or the presence of surfactants. It must be mentioned that PS-NPLs have been engineered and designed to have a perfectly spherical shape, no aggregation, and high stability, as they are produced for commercial purposes and commonly used as reference materials in research. Contrary, PLA-NPLs were lab-made from PLA pellets (Alaraby et al., 2024a).

It is worth mentioning that in previous studies the capability of *D. melanogaster* larvae to ingest huge amounts of all these NPLs was demonstrated, with no effects on the viability. Furthermore, all used NPLs were detected in the midgut lumen, interacting with gut bacteria and with the epithelia cells, crossing the intestinal barrier and resting into the inner parts of the larvae body like the haemolymph, where internalized into the hemocytes (Alaraby et al., 2015, 2022, 2024a). Although these reports were obtaining by feeding larvae, the presence of MNPLs in the intestine of adults has been already reported (Tu et al., 2023). All this suggests that particles in the nano-range have the

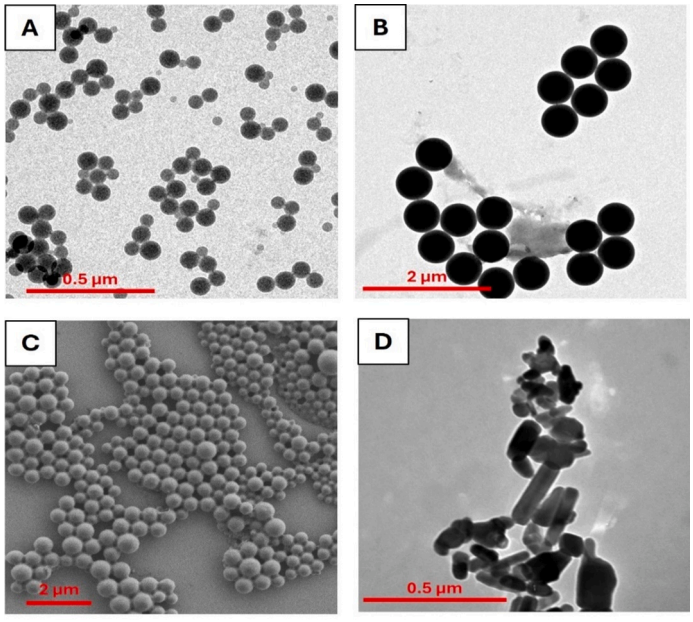

E

	TEM (nm)	Z-aver (d. nm)	PDI	ZP (mV)
PS 50	61.40±14.72	73.74±1.88	0.053±0.006	49.7±0.88
PS 500	415.22±25.25	488.9±8.62	0.083±0.022	53.0±1.99
PLA	463.90±12.94	425.7±10.22	0.257±0.023	16.6±0.80
ZnO	132.37±69.13	114.7±0.86	0.153±0.007	11.4±0.26

Fig. 2. Characterization of the used NPLs and the positive control. (A) TEM image of 50 nm PS-NPLs (PS50). (B) TEM image of 500 nm PS-NPLs (PS500). (C) SEM image of ~300 nm PLA-NPLs. (D) TEM image of ~150 nm ZnO-NPs. (E) Table summarizing the particle diameter in its dry stage (TEM) using the previous images and the ImageJ software; the nanoparticles hydrodynamic size (*Z*-aver) using DLS; the polydispersity index (PDI); and the zeta potential (ZP). Values are indicated as mean ± standard deviation.

potential ability to access a wide range of systems, organs, and tissues and interact with all sorts of surfaces and organisms, including *Drosophila*.

3.2. Visualisation of midgut bacteria and bacteria-NPLs direct interaction

The TEM and SEM images provided an early visualisation of the microorganisms that can be found in the gut of *D. melanogaster*. In Fig. 3, representative images of the bacteria residing in the intestinal lumen are shown. Particularly, in the TEM image of a transversal cut of *Drosophila's* midgut (Fig. 3.A), microorganisms with different morphologies can be observed. After the gut extraction, lysis and homogenization of the samples for bacterial DNA extraction, the presence of bacilli- and coco-shaped bacteria could be confirmed by SEM images (Fig. 3.B). In addition, the ability of 50 nm PS-NPLs to adhere or attach on the bacterial membrane could be captured (Fig. 3.C) as well as its internalization and agglomeration inside the cell (Fig. 3.D). It was already demonstrated the capacity of interaction between both the NPLs (PS and PLA) and the bacteria residing in the midgut of *Drosophila* larvae (Alaraby et al., 2022, 2024a, 2024b).

3.3. Effects of NPLs on the abundance of microorganisms

In this study, the abundance of microorganisms was first determined in two different ways. Firstly, absolute abundance refers to the raw number of individual organisms identified, providing insight into the total quantity of bacteria sequenced in the sample. This measurement gives a direct count of the microbial load present in the sample. The other measurement, relative abundance, presents a more comparative view, illustrating the proportions or ratios at which each species is present in its respective environment. Rather than focusing on total numbers, relative abundance highlights how different species are distributed within the community, offering a more nuanced understanding of how the microbiota is structured across different conditions or treatments.

The analysis of the absolute abundance of gut microorganism revealed notable differences between the control and the treatment groups. From each sample (3 replicates of 50 adult fly guts), the control group reached up to 150,000 bacteria, while the treatments, including those exposed to PLA-NPLs, PS50, PS500, and ZnO-NPs, exhibited a sharp decrease, ending at around 15,000 bacteria after NPL treatments and 50,000 in the ZnO-NP treatment (Fig. 4). This significant reduction in the number of microorganisms can be directly correlated with the treatments applied. Interestingly, the effects induced by the positive control (ZnO-NPs) induce mild effects regarding those induced by the tested NPLs. It is important to point out that no previous studies have been found indicating the absolute number of microorganisms living into the *Drosophila* intestine. Although the extraction procedures do reduce the existing microbiota, including this approach was considered relevant to have a more graphical view of the effects of the exposure on *Drosophila* microbiota, since such reduction would affect all the samples. To overcome the inherent difficulties to interpret absolute number of microorganisms values, the relative abundance of the most abundant species was also determined (Fig. 5).

From the obtained results, two key observations are noteworthy. First, both treatments involving PS-NPLs, regardless of particle size (PS50 and PS500), resulted in similar microbial community compositions. This is consistent with the expectation that since both treatments involve the same agent —polystyrene— their impact on the gut microbiota would be comparable, with size variations having less influence on species composition. Interestingly, PS-NPL degradation into monomers of styrene and oligomers (dimers and trimers) has been described as

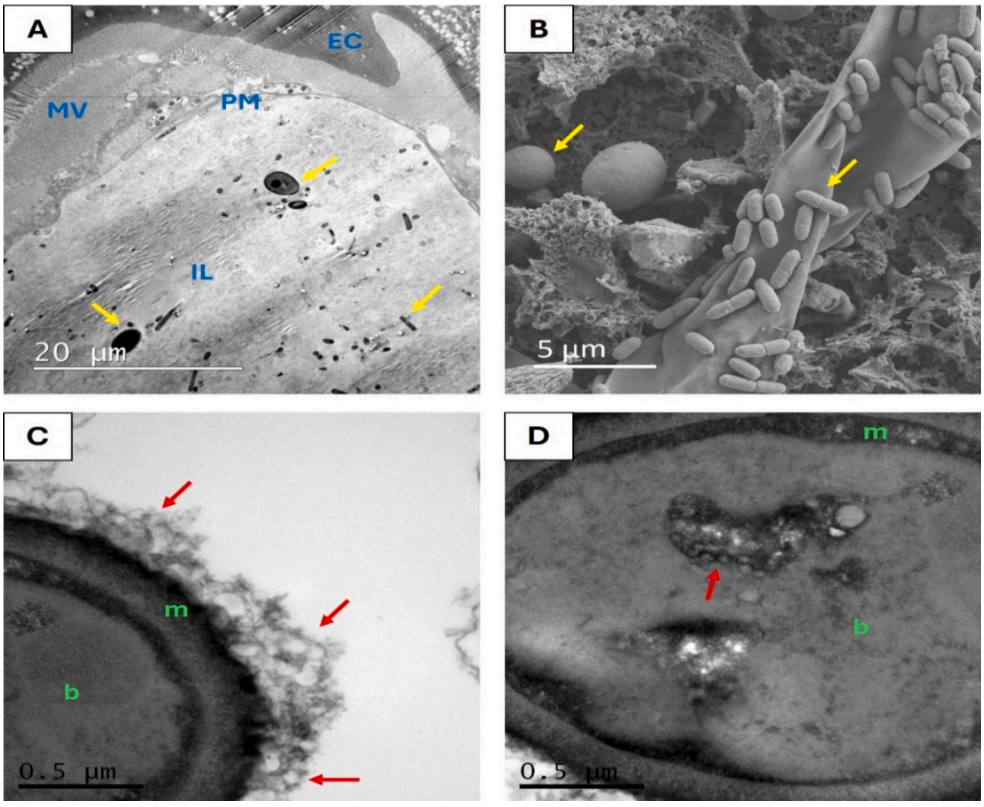

Fig. 3. Microscopy images. (A) TEM images of fly midgut transversal cuts showing the intestinal lumen (IL), the peritrophic membrane (PM), the microvilli structures (MV) of enterocyte cells (EC) forming the intestinal epithelium. Yellow arrows are pointing out the microbiota residing in the midgut lumen. (B) SEM image of intestinal samples homogenized before the bacteria DNA extraction. Yellow arrows indicate the presence of bacilli and coco-shaped bacteria. (C) 50 nm PS-NPL (red arrows) attached/adhered or adsorbed in the membrane (m) of a bacterial cell (b). (D) 50 nm PS-NPL agglomeration inside a bacterial cell (b).

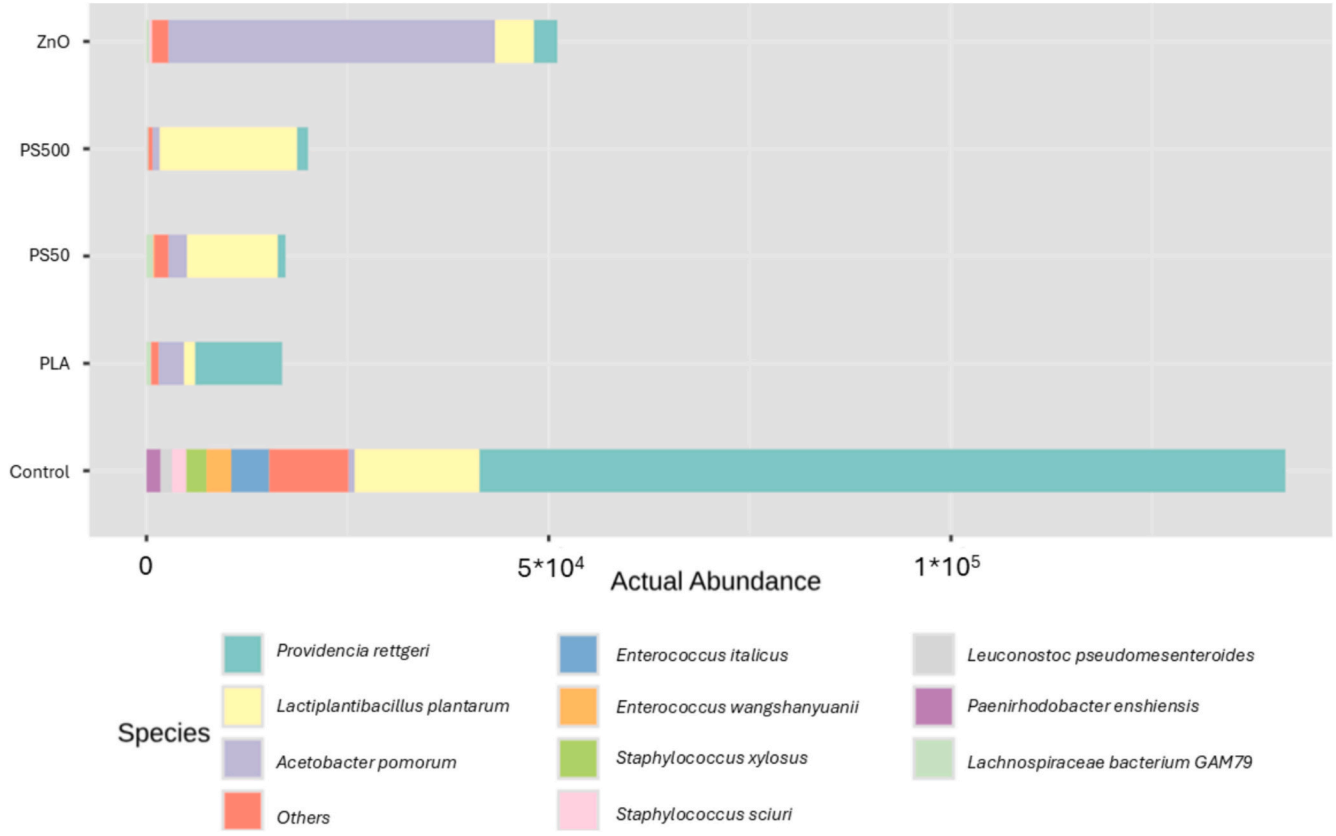

Fig. 4. Absolute abundance. Bar chart depicting absolute abundance of top 10 species across all treatments.

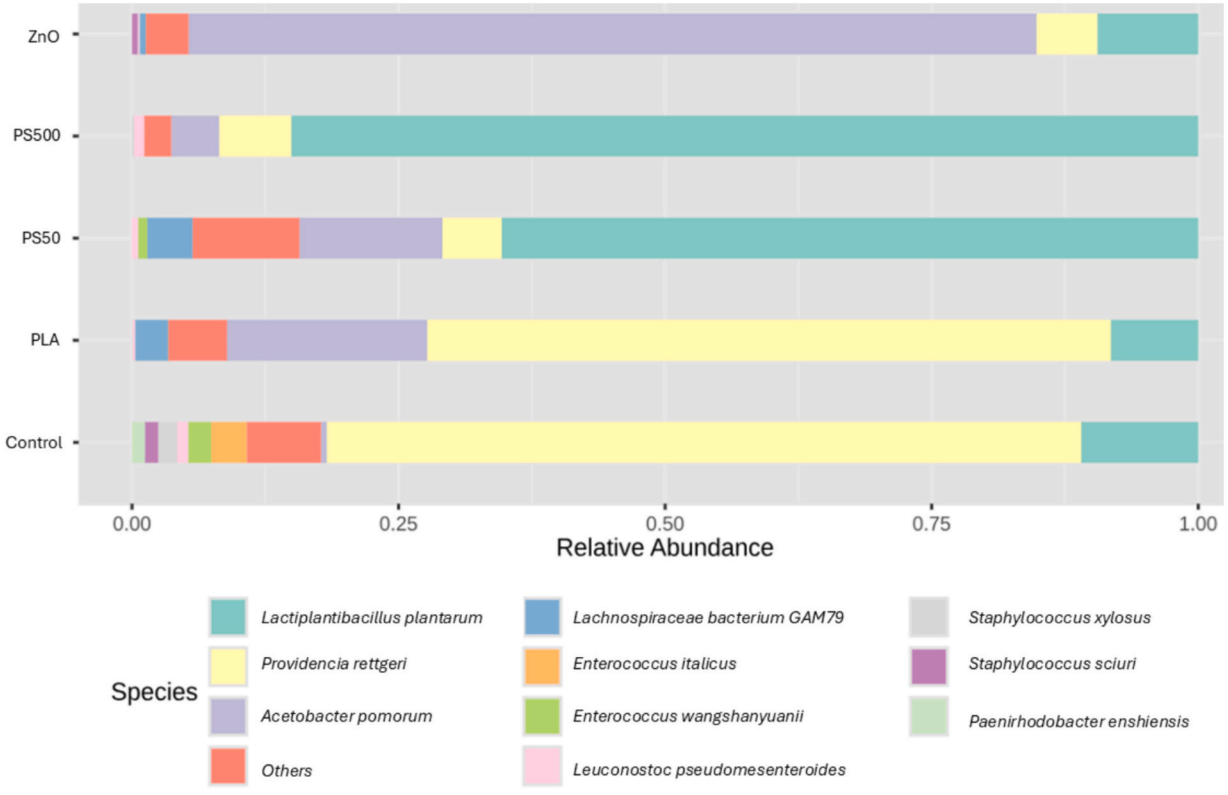

Fig. 5. Relative microbial abundance. Bar chart depicting the relative abundances of the top 10 species across all treatments.

hazardous compounds capable of altering bacterial communities (Tsochatzis et al., 2021; Zhao et al., 2024). For example, when clamworms were fed with PS-NPLs, their decomposition led to significant changes in the gut microbiome, promoting the establishment of novel microbial populations specialized in PS-NPL metabolism, thereby reshaping the microbial community to enhance polymer digestion (Zhao et al., 2024).

Accordingly, secondary by-products of PS-NPLs might have partial responsibility on microbial dysbiosis. However, further research needs to be conducted for clarifications. Secondly, the treatment with polylactic acid (PLA) demonstrated a reduction in microbial composition diversity that was less pronounced, compared to the PS-NPL treatment, but followed a similar trend in terms of the affected species. This suggests that PLA-NPLs, though still causing dysbiosis, may have a relatively milder effect on gut microbiota diversity compared to PS-NPLs. The lower impact of PLA-NPLs on species diversity implies that it might be a less disruptive plastic in terms of microbiota balance, though further research is needed to explore its full range of effects on gut health. In general, PLA has been described to be a bio-compatible polymer since it is made by organic materials like starch-rich crops or rice and sugarcane (Swetha et al., 2023). However, the compatibility of its nano counterparts has been little to not studied in deep. In previous investigations, it was observed that *in vitro* (using the Caco-2/HT29-MTX model) and *in vivo* (using *D. melanogaster* flies) exposures to PLA-NPLs can disrupt the intestinal epithelium (Banaei et al., 2023; Alaraby et al., 2024a).

This observed reduction in the microbial number has been found to compromise the intestinal barrier, leaving it less protected and more susceptible to colonisation by pathogenic bacteria. A weakened microbial community can also increase the vulnerability of the gut to other forms of tissue damage, further impairing gut health and function (Di Tommaso et al., 2021). Similarly, Su and colleagues found that PS-MPLs (25 μm) negatively affected gut microbiota of Kunming mice by reducing microbial diversity, especially in females, with shifts in gut microbiota composition linked to dysbiosis and increased *Prevotellaceae* abundance (Su et al., 2024). In addition, PS-MPL treatments altered the mice intestinal structure, with more pronounced effects in females. Exposures led to decreased villus height, width, and intestinal surface area, along with downregulation of tight junction genes (*claudins* and *occludins*), suggesting impaired gut barrier function (Su et al., 2024).

Research has shown that when microbes are exposed to different MNPLs they exhibit significant reductions in survival and reproduction, alongside increased oxidative stress levels (Huo et al., 2022). This further supports the theory that, in general, MNPLs have

toxic effects on the gut microbiota, disrupting microbial communities and leading to gut dysbiosis. Thus, the oxidative stress caused by MNPLs may lead to cell damage within microbial populations, reducing both microbial diversity and abundance, as observed in this study. Additionally, it is important to consider the broader context of how MNPLs also affect the *Drosophila* model itself. As previously discussed, MNPL exposure impacts *Drosophila* by inducing changes in gut microbiota composition, but the altered physiological state of the host could contribute to these observations as well. Stress responses in the host, such as increased ROS levels and changes in immune function, may exacerbate the harmful effects on the microbiota. According to this, previous results highlighted that although *Drosophila* larvae exposed to different sizes of PS-NPLs did not show any decrease in egg-to-adult survival, larvae presented an increased ROS production and DNA damage in the midgut as well as alterations in genes related to stress, antioxidant response, DNA repair and intestinal damage (Alaraby et al., 2022). Similarly, the exposure to PLA-NPLs triggered oxidative stress, midgut inflammation, structural damage of the midgut epithelium and DNA damage (Alaraby et al., 2024a). Overall, this complex interplay between host and microbiota should be considered when evaluating the full scope of the toxic impact of MNPLs on gut health.

Regarding to the observed blooms and shifts of specific species, it must be pointed out that in the control group the dominant species was *Providencia rettgeri*, a well-documented opportunistic species known to colonize *Drosophila* (Galac and Lazzaro, 2011). This bloom of *Providencia* has already been documented in individual rearing in laboratory conditions (Chandler et al., 2011). In contrast, flies exposed to PS-NPLs primarily harboured *Lactiplantibacillus plantarum*, a species with both beneficial and detrimental effects. *L. plantarum* can promote growth (Storelli et al., 2011) and outcompete harmful species (Gavrilova et al., 2023), yet it is also associated with lifespan reduction in *Drosophila* due to the production of reactive oxygen species (ROS) (Onuma et al., 2023). Another key species identified, *Acetobacter pomorum*, is a known mutualist in the *Drosophila* gut, aiding in protection against invasive species (Hanson et al., 2023) and supplementing the fly's diet (Sannino and Dobson, 2023).

Another relevant observation related to the MNPL effects refers to the microbial cell wall structure, particularly in terms of gram-positive and gram-negative bacteria. Among the three main species identified in the samples, *Lactiplantibacillus plantarum* is gram-positive, while *Providencia rettgeri* and *Acetobacter pomorum* are gram-negative bacteria. In the PS-NPL treatments, *L. plantarum* thrives significantly more compared to the control and other samples, where gram-negative bacteria dominate. This shift in dominance might suggest that the presence of PS-NPLs in the environment could favour somehow the survival and proliferation of gram-positive bacteria like L. *plantarum*. A possible explanation is that the cell wall structure of gram-positive bacteria, which contains a thicker layer of peptidoglycan, may offer greater resistance to the stress or toxic effects induced by PS-NPLs (or MNPLs in general). In contrast, gram-negative bacteria, with their thinner peptidoglycan layer and outer membrane, may be more vulnerable to the interaction of nanoparticles and their effects, leading to a decrease in their prevalence exposed scenarios. This proposal is supported by studies with other materials which show gram-positive bacteria being more resilient to nanomaterials than gram-negative (Heys et al., 2014). This shift in microbial dominance based on cell wall structure underscores the complex interactions between plastic particles and the gut microbiota, where specific traits like gram-positive or gram-negative classification play a role in how bacteria adapt or succumb to the environmental stress caused by MNPLs. Likewise, smaller particles with higher surface area-to-volume ratios are more reactive to their environment and can adsorb any type of molecule facilitating the crossing of bacterial cell membranes, consequently disrupting microbial homeostasis. Additionally, surface charge influences electrostatic interactions, potentially enhancing bacterial adhesion or repelling specific strains (Demarquoy, 2024). These combined factors, influences in shaping the overall composition and functionality of the gut microbiota, highlighting the intricate dynamics between MNPLs and microbial ecosystems. This is a big knowledge gap that remains unresolved, since understanding these interactions is crucial for assessing the long-term impacts of plastic pollution on environmental and host-associated microbiomes.

3.4. Firmicutes/bacteroidetes ratio

When examining species diversity within the gut microbiota, the analysis of the distribution of bacterial phyla provides valuable insights. In *D. melanogaster*, the gut microbiota is predominantly composed of three major phyla: *Proteobacteria*, which typically account for approximately 70 % of the community; *Firmicutes*, representing around 20 %; and *Bacteroidetes*, comprising roughly 10 %. This distribution reflects the characteristic microbial composition of *Drosophila* and serves as a baseline for understanding changes induced by environmental factors or experimental treatments. (Chen et al., 2022). This is particularly significant because the ratio between *Firmicutes* and *Bacteroidetes* (F/B ratio) is considered one of the most relevant and used biomarkers in gut microbiota studies. This ratio reflects the balance of key bacterial groups involved in nutrient acquisition and metabolism. A lower F/B ratio has

often been associated with various diseases and disorders in humans, highlighting its potential as an indicator of gut health and dysbiosis (An et al., 2023). In *Drosophila*, the F/B ratio typically fluctuates but generally remains around 250 (Ji et al., 2022). As depicted in Fig. 6, the F/B ratios for all samples clearly illustrate the impact of NPL treatments on the gut microbiota of *Drosophila* flies. The observed reductions in this ratio compared to the control further support the conclusion that exposure to MNPLs induces significant changes in microbial community composition. Similarly, previous studies have demonstrated that exposures to PS-MPLs (0.5, 5, and 50 μm) also decrease the amount of firmicutes present in caecal and faecal samples of different organisms like mice, and/or Chinese mitten crab (Lu et al., 2018; Jin et al., 2019; Liu et al., 2019; Sun et al., 2021). However, other studies have reported that in zebrafish the phylum *Firmicutes* increases when exposed to PS-MPLs (0.5, 5, and 50 μm), while the *Bacteroidetes* decreases (Jin et al., 2018; Wan et al., 2019).

3.5. Microbial diversity

Another important element to check in microbiota analysis is the alpha diversity, which is a frequently employed metric that accounts for all uniquely identified taxa within a sample, providing insight into both the diversity and richness of species present. In this study, Chao1 was used as the biodiversity index to estimate species richness, and the Kruskal-Wallis's test was applied for statistical analysis. As shown in Fig. 7, these results indicate that, despite observed variability within samples, there is a significant decrease in overall diversity from the control group to all treatment groups.

A well-balanced microbiota is a fundamental component of disease prevention. In a healthy individual, the gut microbiota plays a crucial role in nutrient extraction by producing enzymes that the host cannot synthesize. Additionally, it provides protection against pathogens through competitive exclusion and the production of antimicrobial compounds. While the precise definition of a "healthy microbiota" remains a topic of debate, it is generally characterized by high taxonomic diversity, rich gene content, and overall stability (McBurney et al., 2019)

These findings could suggest that MNPLs significantly reduce species diversity within the gut microbiota of *D. melanogaster*, mirroring the effects of the bactericidal agent ZnO-NPs. This reduction in microbial diversity indicates that MNPLs can induce severe dysbiosis, disrupting the balance of the gut microbiota. Such alterations in microbial composition are associated with a range of adverse effects on the host, including diverse diseases (irritable and inflammatory bowel disease) and metabolic disorders (obesity, diabetes) (Jandhyala et al., 2015; Hills Jr et al., 2019). Similarly, other studies also found that exposing other model organisms like bees to PS-MPLs decreases the alpha diversity of their microbiome (Wang et al., 2022). Interestingly, reduced alpha diversity was also observed in human microbiota after exposure to polyethylene terephthalate (PET) MPLs using a model simulating gastrointestinal digestion (Tamargo et al., 2022).

3.6. Community diversity

Furthermore, the microbial Beta-diversity metric of the exposed fly's population has also been investigated. Beta diversity quantifies the variation or differences in microbial communities across different samples. It enables the comparison of factors such as relative abundance and species composition under different environmental or experimental conditions. In this study, beta-diversity was calculated using the Bray-Curtis index as the dissimilarity measure, PERMANOVA as the statistical method and Nonmetric Multidimensional Scaling (NMDS) was used as the ordination method. The results are presented in Fig. 8.

Two key results emerge from this analysis. Firstly, the control group exhibited significant similarity across all three replicates, indicating a stable and consistent microbial community in adult flies making it a suitable model to study variations or differences in microbial communities among treatments. Secondly, all treatment groups showed an increased distance between replicates, suggesting that the microbial communities in these groups are less stable and experience greater changes and species turnover when exposed to the selected NPLs and ZnO-NPs. These findings would indicate that exposures to the selected NPLs and ZnO-NPs destabilises the gut microbiota, leading to more variable and easily replaceable microbial communities compared to those in healthy flies. It is important to remark how the ZnO treatment shows a more stable community compared to the MNPLs treatments, meaning that the negative control has less of an effect in microbiota stability that the plastic themselves. Resembling results were found when studying the effects of 20, 500, and 5000 nm PS-NPLs in BALB/c mice for 14 and 28 days. In such study the authors revealed a distinct PCA (principal component analysis) separation between the gut microbiota of treated groups than the control group (Zhang et al., 2023).

Altogether, these results suggest that the gut microbiota affected by

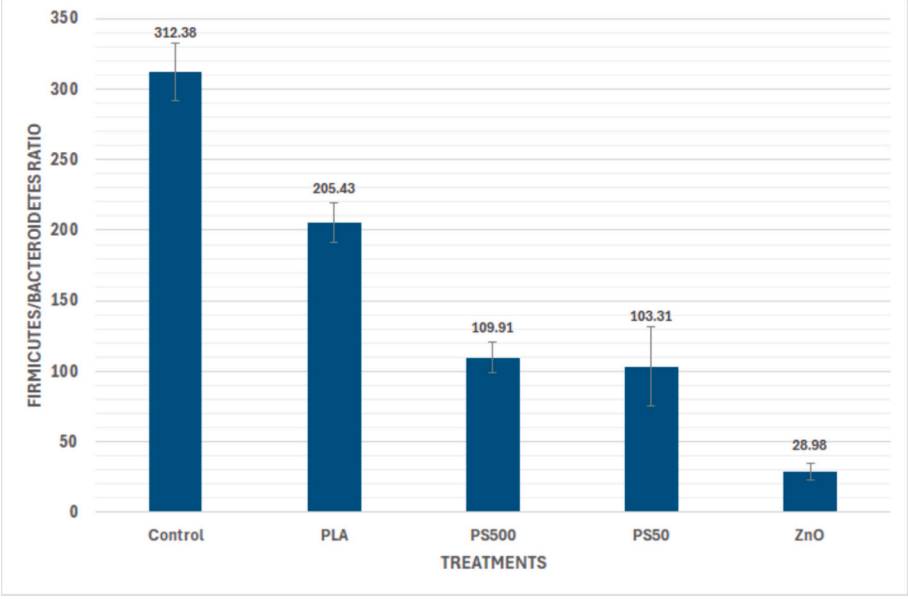

Fig. 6. Firmicutes/Bacteroidetes ratio across all treatments.

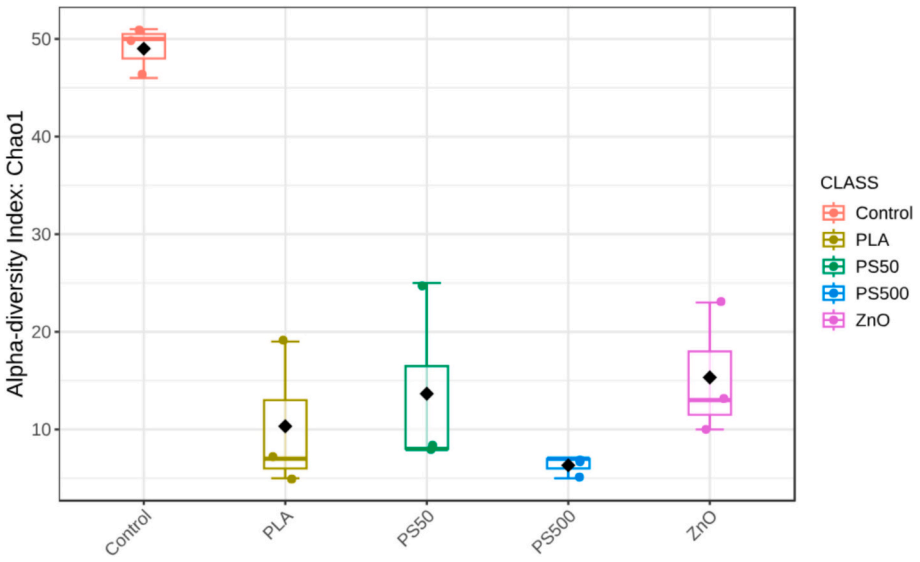

Fig. 7. Dot plot depicting alpha diversity across all treatments. *p*-values: Control-PLA-NPLs, Control-PS50, Control-PS500, Control-ZnO-NPs $\leq$ 0.05. Between treatments $\geq$0.05. Chao1 was used as the diversity index and Kruskal-Wallis as the statistical method.

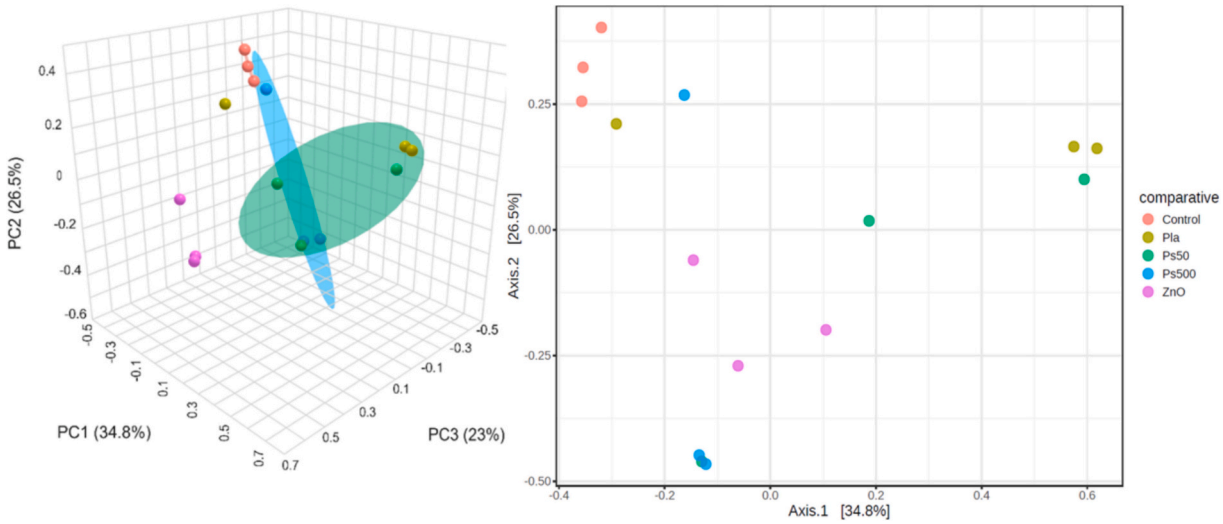

Fig. 8. PCoA plot (2D and 3D) representing beta diversity between all treatments, Bray-Curtis as the statistical comparison and PERMANOVA as the statistical method. *p*-value = 0.002.

MNPLs experiences not only a reduction in species diversity but also an increased susceptibility to shifts in microbial composition. This instability makes the gut environment less resilient and more vulnerable to colonisation by pathogenic microorganisms, further compromising the host's health and increasing the risk of infection (Chopyk and Grakoui, 2020).

3.7. LEfSe analysis

Further, a Linear Discriminant Analysis Effect Size (LefSe) analysis was conducted at the species level. LefSe is a robust algorithm for multidimensional biomarker discovery, specifically designed to identify taxa with significant differential abundances across experimental conditions or biological factors. The method integrates a Kruskal-Wallis (KW) sum-rank test to detect taxa with statistically significant differences in abundance, followed by Linear Discriminant Analysis (LDA) to quantify the effect size of these differentially abundant features.

As shown in Fig. 9, several species exhibited significant changes in abundance, all of which were more prevalent in the control group. This analysis might serve as a reliable tool to detect biomarkers of MNPLs susceptibility. Since in this case all treatments drastically diminished the total and relative abundance of bacterial content compared to the control, no species were found standing out over the general population. For example, although some of the species indicated in Fig. 9, such as *Staphylococcus sciuri*, have shown to be associated with disease, they do not serve as reliable markers for analysis due to their low abundance.

Finally, Table 1 summarizes all the results obtained in this study, using a heatmap design to visually represent the significance of the findings and their direction (increase or decrease compared to the control group). This approach provides a clear and intuitive overview of the observed effects.

Based on the data, it can be concluded that the used NPLs exhibit behavior like—or at least show trends comparable with—the well-established biocide and antimicrobial agent, zinc oxide nanoparticles (ZnO-NPs). ZnO-NPs are known for their potent antimicrobial effects, primarily through the generation of reactive oxygen species (ROS) and disruption of microbial cell membranes, making them highly effective against a broad spectrum of bacteria and fungi (Gökmen et al., 2024).

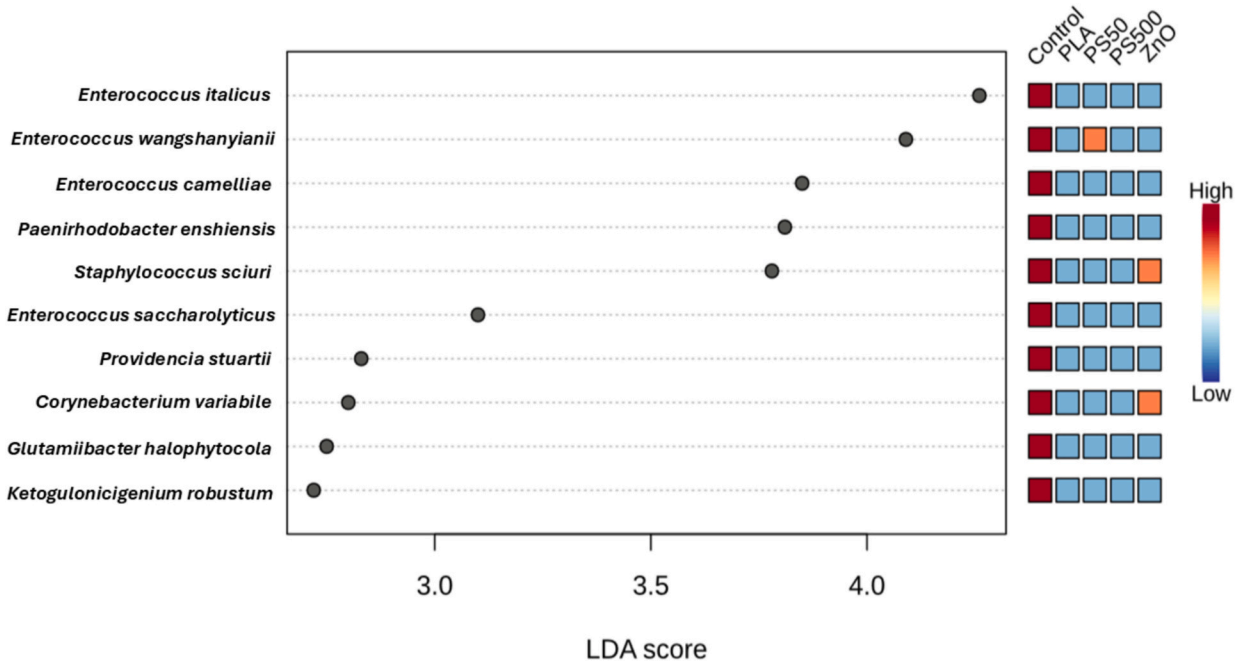

Fig. 9. LEfSe of different species. Relative abundance is significant when *p*-value ≤0.05 and logarithmic LDA score ≥ 2. LDA; Linear Discriminant Analysis.

Table 1
Comparisons of main markers between treatments. Alpha diversity is measured by Chao1 index. Beta diversity is calculated by the Bray-Curtis index as the dissimilarity between pools from different conditions. Values are compared to the control group (*$p \leq 0.05$, **$p \leq 0.01$, *** $p \leq 0.001$).

Treatment	Total abundance	Main species	F/B ratio	Alpha diversity	Beta diversity
Control	138,437	*P. rettgeri* (Gram-)	312.38	48.96	0.52
PLA	16,867 ***	*P. rettgeri* (Gram-)	205.43 *	10.26 **	5.18 *
PS500	20,080 ***	*L. plantarum* (Gram+)	109.91 **	6.28 **	6.74 *
PS50	17,296 ***	*L. plantarum* (Gram+)	103.31 **	13.74 **	4.38 *
ZnO	51,042 **	*A. pomorum* (Gram-)	28.98 ***	15.03 **	4.11 *

These properties have led to their widespread use in consumer products such as cosmetics, food packaging, and textiles, where they inhibit microbial growth and enhance product safety and durability (Gulab et al., 2024).

It is worth noting that PLA (a bio-based polymer specifically designed to exhibit greater biocompatibility with the surrounding environment) appears to have a slightly less pronounced impact on microbial communities, particularly when analyzing the dominant species and the Firmicutes-to-Bacteroidetes (F/B) ratio (Table 1). However, the results from other analyses indicate that PLA-NPLs exhibit similar behavior to both PS-NPLs and ZnO-NPs. For this reason, a holistic assessment of all the parameters analyzed is crucial to extracting more robust and reliable conclusions. Focusing on a single metric, such as the F/B ratio, may overlook broader trends or subtle variations that emerge when considering the full range of data. By integrating findings across multiple analyses, the interpretation of the results becomes more comprehensive and increases the reliability of the study's conclusions.

4. Conclusions

The gut microbiota has recently garnered significant attention due to the growing understanding of its crucial role in human health. Simultaneously, MNPLs have emerged as of prominent environmental concern, being labelled as pollutants due to their persistence and harmful effects on both ecosystems and human health. This study, successes using *Drosophila* as a model organism for microbiota analysis and employing nanopore sequencing as a key tool for profiling the microbial community (or microbiome). Accordingly, this investigation focused on understanding the impact of MNPLs on the gut microbiota of *Drosophila.*

Results indicate that various polymers, including PS (a petroleum-based polymer) and PLA (a bio-based polymer), exerted similar overall effects on the microbiota while having some differences between them. Specifically, PS-NPLs were found to cause a greater alteration in microbiota diversity compared to PLA-NPLs. Additionally, it was shown that PS-NPLs of different sizes yielded similar effects on the microbiome. In all cases, exposure to these MNPLs induced dysbiosis, resulting in a reduction in both the diversity and richness of the *Drosophila* gut microbiome.

However, further research is needed to fully elucidate the mechanisms underlying the interactions between MNPLs and microorganisms. The exact mechanisms and interactions of MNPLs on microbial communities, including the influence of factors such as particle size and polymer composition, remain unclear and are subjects of ongoing debate. Additionally, the potential impact of MNPLs on the gut epithelium also warrants further investigation since it can be an indirect way of MNPLs to dysregulate the residing microbial communities. Given the increasing concern about the health implications of MNPLs, it is crucial to implement direct regulatory actions from governments and public health institutions to regulate the production and use of plastic materials, mainly those of single use. Concurrently, more research is required to explore viable alternatives to plastics and to develop new models for studying their effects on both environmental and human health.

CRediT authorship contribution statement

Arnau Rocabert: Writing – original draft, Conceptualization. **Joan Martín-Pérez:** Conceptualization. **Laia Pareras:** Investigation. **Raquel Egea:** Data curation. **Mohamed Alaraby:** Methodology. **Jordi Manuel Cabrera-Gumbau:** Formal analysis. **Iris Sarmiento:** Formal analysis. **Jaime Martínez-Urtaza:** Supervision, Funding acquisition, Formal

analysis. **Laura Rubio:** Supervision, Investigation. **Irene Barguilla:** Supervision, Investigation. **Ricard Marcos:** Writing – review & editing, Conceptualization. **Alba García-Rodríguez:** Writing – review & editing, Supervision, Conceptualization. **Alba Hernández:** Writing – review & editing, Funding acquisition, Conceptualization.

Declaration of competing interest

The authors declare that they have no known competing financial interests or personal relationships that could have appeared to influence the work reported in this paper.

Acknowledgments

AR and JMP hold Ph.D. fellowships from the Generalitat de Catalunya. AGR (Academic record 2020 BP 00177), MA (Academic record 2022 BP 00026), and IB (Academic record 2023 BP 00212) were granted with a Beatriu de Pinós Postdoctoral Program from the Secretariat of Universities and Research of the Department of Business and Knowledge of the Government of Catalunya. AH was granted an ICREA ACADEMIA award. This project (PlasticHeal) has received funding from the European Union's Horizon 2020 - Research and Innovation Framework Programme under grant agreement No 965196. This work was partially supported by the Spanish Ministry of Science and Innovation [PID2020-116789, RB-C43] and the Generalitat de Catalunya (2021-SGR-00731 and 2021-SGR-00526).

Appendix A. Supplementary data

Supplementary data to this article can be found online at https://doi.org/10.1016/j.scitotenv.2025.179545.

Data availability statement

The raw ONT data for each individual sample was deposited in the SRA under the BioProject accession number PRJNA1235641. Additional information can be made available from the authors upon request.

References

Alaraby, M., Annangi, B., Hernández, A., Creus, A., Marcos, R., 2015. A comprehensive study of the harmful effects of ZnO nanoparticles using *Drosophila melanogaster* as an *in vivo* model. J. Hazard. Mater. 296, 166–174. https://doi.org/10.1016/j.jhazmat.2015.04.053.

Alaraby, M., Abass, D., Domenech, J., Hernández, A., Marcos, R., 2022. Hazard assessment of ingested polystyrene nanoplastics in *Drosophila* larvae. Environ. Sci. Nano 9, 1845–1857. https://doi.org/10.1039/d1en01199e.

Alaraby M, Villacorta A, Abass D, Hernández A, Marcos R. The hazardous impact of true-to-life PET nanoplastics in *Drosophila.* Sci. Total Environ., 2023, 63, 160954 (2023). doi: https://doi.org/10.1016/j.scitotenv.2022.160954.

Alaraby, M., Abass, D., Farre, M., Hernández, A., Marcos, R., 2024a. Are bioplastics safe? Hazardous effects of polylactic acid (PLA) nanoplastics in Drosophila. Sci. Total Environ. 919, 170592. https://doi.org/10.1016/j.scitotenv.2024.170592.

Alaraby, M., Abass, D., Gutiérrez, J., Hernández, A., Marcos, R., 2024b. Reproductive toxicity of nanomaterials using silver nanoparticles and *Drosophila* as models. Molecules 29 (23), 5802. https://doi.org/10.3390/molecules29235802.

An, J., Kwon, H., Kim, Y.J., 2023. The Firmicutes/Bacteroidetes ratio as a risk factor of breast cancer. J. Clin. Med. 12 (6), 2216. https://doi.org/10.3390/jcm12062216.

Banaei, G., García-Rodríguez, A., Tavakolpournegari, A., Martín-Pérez, J., Villacorta, A., Marcos, R., Hernández, A., 2023. The release of polylactic acid nanoplastics (PLA-NPLs) from commercial teabags. Obtention, characterization, and hazard effects of true-to-life PLA-NPLs. J. Hazard. Mater. 458, 131899. https://doi.org/10.1016/j.jhazmat.2023.131899.

Beribaka, M., Jelić, M., Tanasković, M., Lazić, C., Stamenković-Radak, M., 2021. Life history traits in two *Drosophila* species differently affected by microbiota diversity under lead exposure. Insects 12 (12), 1122. https://doi.org/10.3390/insects12121122.

Campana, A.M., Laue, H.E., Shen, Y., Shrubsole, M.J., Baccarelli, A.A., 2022. Assessing the role of the gut microbiome at the interface between environmental chemical exposures and human health: current knowledge and challenges. Environ. Pollut. 315, 120380. https://doi.org/10.1016/j.envpol.2022.120380.

Chandler, J.A., Lang, J.M., Bhatnagar, S., Eisen, J.A., Kopp, A., 2011. Bacterial communities of diverse *Drosophila* species: ecological context of a host-microbe model system. PLoS Genet. 7 (9), e1002272. https://doi.org/10.1371/journal.pgen.1002272.

Chen, J.S., Tsaur, S.C., Ting, C.T., Fang, S., 2022. Dietary utilization drives the differentiation of gut bacterial communities between specialist and generalist Drosophilid flies. Microbiol. Spectr. 10 (4), e0141822. https://doi.org/10.1128/spectrum.01418-22.

Chopyk, D.M., Grakoui, A., 2020. Contribution of the intestinal microbiome and gut barrier to hepatic disorders. Gastroenterology 159 (3), 849–863. https://doi.org/10.1053/j.gastro.2020.04.077.

Curry, K.D., Wang, Q., Nute, M.G., Tyshaieva, A., Reeves, E., Soriano, S., Wu, Q., Graeber, E., Finzer, P., Mendling, W., Savidge, T., Villapol, S., Dilthey, A., Treangen, T.J., 2022. Emu: species-level microbial community profiling of full-length 16S rRNA Oxford Nanopore sequencing data. Nat. Methods 19 (7), 845–853. https://doi.org/10.1038/s41592-022-01520-4.

D'Argenio, V., Salvatore, F., 2015. The role of the gut microbiome in the healthy adult status. Clin. Chim. Acta 451 (Pt A), 97–102. https://doi.org/10.1016/j.cca.2015.01.003.

De Coster, W., Rademakers, R., 2023. NanoPack2: population-scale evaluation of long-read sequencing data. Bioinformatics 39 (5), btad311. https://doi.org/10.1093/bioinformatics/btad311.

Demarquoy, J., 2024. Microplastics and microbiota: unraveling the hidden environmental challenge. World J. Gastroenterol. 30 (16), 2191–2194. https://doi.org/10.3748/wjg.v30.i16.2191.

Dhariwal, A., Chong, J., Habib, S., King, I.L., Agellon, L.B., Xia, J., 2017. MicrobiomeAnalyst: a web-based tool for comprehensive statistical, visual and meta-analysis of microbiome data. Nucleic Acids Res. 45 (W1), W180–W188. https://doi.org/10.1093/nar/gkx295.

Di Tommaso, N., Gasbarrini, A., Ponziani, F.R., 2021. Intestinal barrier in human health and disease. Int. J. Environ. Res. Public Health 18 (23), 12836. https://doi.org/10.3390/ijerph182312836.

Dominguez-Bello, M.G., Godoy-Vitorino, F., Knight, R., Blaser, M.J., 2019. Role of the microbiome in human development. Gut 68 (6), 1108–1114. https://doi.org/10.1136/gutjnl-2018-317503.

Dong, Y., Ding, Z., Song, L., Zhang, D., Xie, C., Zhang, S., Feng, L., Liu, H., Pang, Q., 2022. Sodium benzoate delays the development of *Drosophila melanogaster* larvae and alters commensal microbiota in adult flies. Front. Microbiol. 13, 911928. https://doi.org/10.3389/fmicb.2022.911928.

Galac, M.R., Lazzaro, B.P., 2011. Comparative pathology of bacteria in the genus *Providencia* to a natural host. Drosophila melanogaster. Microbes Infect. 13 (7), 673–683. https://doi.org/10.1016/j.micinf.2011.02.005.

Gavrilova, E., Kostenko, V., Zadorina, I., Khusnutdinova, D., Yarullina, D., Ezhkova, A., Bogachev, M., Kayumov, A., Nikitina, E., 2023. Repression of *Staphylococcus aureus* and *Escherichia coli* by *Lactiplantibacillus plantarum* strain AG10 in *Drosophila melanogaster in vivo* model. Microorganisms 11 (5), 1297. https://doi.org/10.3390/microorganisms11051297.

Gökmen, G.G., Mirsafi, F.S., Leißner, T., Akan, T., Mishra, Y.K., Kışla, D., 2024. Zinc oxide nanomaterials: safeguarding food quality and sustainability. Compr. Rev. Food Sci. Food Saf. 23 (6), e70051. https://doi.org/10.1111/1541-4337.70051.

Gomaa, E.Z., 2020. Human gut microbiota/microbiome in health and diseases: a review. Antonie Van Leeuwenhoek 113 (12), 2019–2040. https://doi.org/10.1007/s10482-020-01474-7.

Gulab, H., Fatima, N., Tariq, U., Gohar, O., Irshad, M., Zubair Khan, M., Saleem, M., Ghaffar, A., Hussain, M., Jan, A.K., Humayun, M., Motola, M., Hanif, M.B., 2024. Advancements in zinc oxide nanomaterials: synthesis, properties, and diverse applications. Nano-Struct. Nano-Objects 39, 101271. https://doi.org/10.1016/j.nanoso.2024.101271.

Hanson, M.A., Grollmus, L., Lemaitre, B., 2023. Ecology-relevant bacteria drive the evolution of host antimicrobial peptides in *Drosophila*. Science 381 (6655), eadg5725. https://doi.org/10.1126/science.adg5725.

Heys, K.A., Riding, M.J., Strong, R.J., Shore, R.F., Pereira, M.G., Jones, K.C., Semple, K.T., Martin, F.L., 2014. Mid-infrared spectroscopic assessment of nanotoxicity in gram-negative *vs* gram-positive bacteria. Analyst 139 (5), 896–905. https://doi.org/10.1039/c3an01649h.

Hills Jr., R.D., Pontefract, B.A., Mishcon, H.R., Black, C.A., Sutton, S.C., Theberge, C.R., 2019. Gut microbiome: profound implications for diet and disease. Nutrients 11 (7), 1613. https://doi.org/10.3390/nu11071613.

Huo, Y., Dijkstra, F.A., Possell, M., Singh, B., 2022. Ecotoxicological effects of plastics on plants, soil fauna and microorganisms: a meta-analysis. Environ. Pollut. 310, 119892. https://doi.org/10.1016/j.envpol.2022.119892.

Jandhyala, S.M., Talukdar, R., Subramanyam, C., Vuyyuru, H., Sasikala, M., Nageshwar, Reddy D., 2015. Role of the normal gut microbiota. World J. Gastroenterol. 21 (29), 8787–8803. https://doi.org/10.3748/wjg.v21.i29.8787.

Ji, D., Sun, H., Yang, W., Gao, M., Xu, H., 2022. Transfer of human microbiome to *Drosophila* gut model. Microorganisms 10 (3), 553. https://doi.org/10.3390/microorganisms10030553.

Jin, Y., Xia, J., Pan, Z., Yang, J., Wang, W., Fu, Z., 2018. Polystyrene microplastics induce microbiota dysbiosis and inflammation in the gut of adult zebrafish. Environ. Pollut. 235, 322–329. https://doi.org/10.1016/j.envpol.2017.12.088.

Jin, Y., Lu, L., Tu, W., Luo, T., Fu, Z., 2019. Impacts of polystyrene microplastic on the gut barrier, microbiota and metabolism of mice. Sci. Total Environ. 649, 308–317. https://doi.org/10.1016/j.scitotenv.2018.08.353.

Johnson, J.S., Spakowicz, D.J., Hong, B.Y., Petersen, L.M., Demkowicz, P., Chen, L., Leopold, S.R., Hanson, B.M., Agresta, H.O., Gerstein, M., Sodergren, E., Weinstock, G.M., 2019. Evaluation of 16S rRNA gene sequencing for species and strain-level microbiome analysis. Nat. Commun. 10 (1), 5029. https://doi.org/10.1038/s41467-019-13036-1.

Klappenbach, J.A., Saxman, P.R., Cole, J.R., Schmidt, T.M., 2001. Rrndb: the ribosomal RNA operon copy number database. Nucleic Acids Res. 29 (1), 181–184. https://doi.org/10.1093/nar/29.1.181.

Liu, Z., Yu, P., Cai, M., Wu, D., Zhang, M., Chen, M., Zhao, Y., 2019. Effects of microplastics on the innate immunity and intestinal microflora of juvenile *Eriocheir sinensis*. Sci. Total Environ. 685, 836–846. https://doi.org/10.1016/j.scitotenv.2019.06.265.

Lu, L., Wan, Z., Luo, T., Fu, Z., Jin, Y., 2018. Polystyrene microplastics induce gut microbiota dysbiosis and hepatic lipid metabolism disorder in mice. Sci. Total Environ. 631-632, 449–458. https://doi.org/10.1016/j.scitotenv.2018.03.051.

McBurney, M.I., Davis, C., Fraser, C.M., Schneeman, B.O., Huttenhower, C., Verbeke, K., Walter, J., Latulippe, M.E., 2019. Establishing what constitutes a healthy human gut microbiome: state of the science, regulatory considerations, and future directions. J. Nutr. 149 (11), 1882–1895. https://doi.org/10.1093/jn/nxz154.

NanoGenotox. Final protocol for producing suitable manufactured nanomaterial exposure media. Nanogenotox, towards a method for detecting the potential genotoxicity of nanomaterials, 2011. https://www.anses.fr/en/system/files/nanogenotox_deliverable_5. pdf.

Niu, H., Liu, S., Jiang, Y., Hu, Y., Li, Y., He, L., Xing, M., Li, X., Wu, L., Chen, Z., Wang, X., Lou, X., 2023. Are microplastics toxic? A review from eco-toxicity to effect s on the gut microbiota. Metabolites 13 (6), 739. https://doi.org/10.3390/metabo13060739.

O'Leary, N.A., Wright, M.W., Brister, J.R., Ciufo, S., Haddad, D., McVeigh, R., Rajput, B., Robbertse, B., Smith-White, B., Ako-Adjei, D., Astashyn, A., Badretdin, A., Bao, Y., Blinkova, O., Brover, V., Chetvernin, V., Choi, J., Cox, E., Ermolaeva, O., Farrell, C. M., Goldfarb, T., Gupta, T., Haft, D., Hatcher, E., Hlavina, W., Joardar, V.S., Kodali, V.K., Li, W., Maglott, D., Masterson, P., McGarvey, K.M., Murphy, M.R., O'Neill, K., Pujar, S., Rangwala, S.H., Rausch, D., Riddick, L.D., Schoch, C., Shkeda, A., Storz, S.S., Sun, H., Thibaud-Nissen, F., Tolstoy, I., Tully, R.E., Vatsan, A. R., Wallin, C., Webb, D., Wu, W., Landrum, M.J., Kimchi, A., Tatusova, T., DiCuccio, M., Kitts, P., Murphy, T.D., Pruitt, K.D., 2016. Reference sequence (RefSeq) database at NCBI: current status, taxonomic expansion, and functional annotation. Nucleic Acids Res. 44 (D1), D733–D745. https://doi.org/10.1093/nar/gkv1189.

Onuma, T., Yamauchi, T., Kosakamoto, H., Kadoguchi, H., Kuraishi, T., Murakami, T., Mori, H., Miura, M., Obata, F., 2023. Recognition of commensal bacterial peptidoglycans defines *Drosophila* gut homeostasis and lifespan. PLoS Genet. 19 (4), e1010709. https://doi.org/10.1371/journal.pgen.1010709.

Sannino, D.R., Dobson, A.J., 2023. *Acetobacter pomorum* in the *Drosophila* gut microbiota buffers against host metabolic impacts of dietary preservative formula and batch variation in dietary yeast. Appl. Environ. Microbiol. 89 (10), e0016523. https://doi.org/10.1128/aem.00165-23.

Sender, R., Fuchs, S., Milo, R., 2016. Revised estimates for the number of human and bacteria cells in the body. PLoS Biol. 14 (8), e1002533. https://doi.org/10.1371/journal.pbio.1002533.

Souza-Silva, T.G., Oliveira, I.A., Silva, G.G.D., Giusti, F.C.V., Novaes, R.D., Paula, H.A.A., 2022. Impact of microplastics on the intestinal microbiota: a systematic review of preclinical evidence. Life Sci. 294, 120366. https://doi.org/10.1016/j.lfs.2022.120366.

Storelli, G., Defaye, A., Erkosar, B., Hols, P., Royet, J., Leulier, F., 2011. *Lactobacillus plantarum* promotes *Drosophila* systemic growth by modulating hormonal signals through TOR-dependent nutrient sensing. Cell Metab. 14 (3), 403–414. https://doi.org/10.1016/j.cmet.2011.07.012.

Su, Q.L., Wu, J., Tan, S.W., Guo, X.Y., Zou, D.Z., Kang, K., 2024. The impact of microplastics polystyrene on the microscopic structure of mouse intestine, tight junction genes and gut microbiota. PLoS One 19 (6), e0304686. https://doi.org/10.1371/journal.pone.0304686.

Sun, H., Chen, N., Yang, X., Xia, Y., Wu, D., 2021. Effects induced by polyethylene microplastics oral exposure on colon mucin release, inflammation, gut microflora composition and metabolism in mice. Ecotoxicol. Environ. Saf. 220, 112340. https://doi.org/10.1016/j.ecoenv.2021.112340.

Sun, Y., Tang, Y., Xu, X., Hu, K., Zhang, Z., Zhang, Y., Yi, Z., Zhu, Q., Xu, R., Zhang, Y., Liu, Z., Liu, X., 2020. Lead exposure results in defective behavior as well as alteration of gut microbiota composition in flies and their offsprings. Int. J. Dev. Neurosci. 80 (8), 699–708. https://doi.org/10.1002/jdn.10067.

Swetha, T.A., Bora, A., Mohanrasu, K., Balaji, P., Raja, R., Ponnuchamy, K., Muthusamy, G., Arun, A., 2023. A comprehensive review on polylactic acid (PLA) -synthesis processing and application in food packaging. Int. J. Biol. Macromol. 234, 123715. https://doi.org/10.1016/j.ijbiomac.2023.123715.

Tamargo, A., Molinero, N., Reinosa, J.J., Alcolea-Rodriguez, V., Portela, R., Bañares, M. A., Fernández, J.F., Moreno-Arribas, M.V., 2022. PET microplastics affect human gut microbiota communities during simulated gastrointestinal digestion, first evidence of plausible polymer biodegradation during human digestion. Sci. Rep. 12 (1), 528. https://doi.org/10.1038/s41598-021-04489-w.

Tsochatzis, E., Berggreen, I.E., Tedeschi, F., Ntrallou, K., Gika, H., Corredig, M., 2021. Gut microbiome and degradation product formation during biodegradation of expanded polystyrene by mealworm larvae under different feeding strategies. Molecules 26 (24), 7568. https://doi.org/10.3390/molecules26247568.

Tu, Q., Deng, J., Di, M., Lin, X., Chen, Z., Li, B., Tian, L., 2023. Zhang Y reproductive toxicity of polystyrene nanoplastics in *Drosophila melanogaster* under multi-generational exposure. Chemosphere 330, 138724. https://doi.org/10.1016/j.chemosphere.2023.138724.

Wan, Z., Wang, C., Zhou, J., Shen, M., Wang, X., Fu, Z., Jin, Y., 2019. Effects of polystyrene microplastics on the composition of the microbiome and metabolism in larval zebrafish. Chemosphere 217, 646–658. https://doi.org/10.1016/j.chemosphere.2018.11.070.

Wang, S., Shi, W., Huang, Z., Zhou, N., Xie, Y., Tang, Y., Hu, F., Liu, G., Zheng, H., 2022. Complete digestion/biodegradation of polystyrene microplastics by greater wax moth (*galleria mellonella*) larvae: direct *in vivo* evidence, gut microbiota independence, and potential metabolic pathways. J. Hazard. Mater. 423 (Pt B), 127213. https://doi.org/10.1016/j.jhazmat.2021.127213.

Wāng Y, Jiang Y. Drosophila melanogaster as a tractable eco-environmental model to unravel the toxicity of micro- and nanoplastics. Environ. Int. 2024 Oct;192:109012. doi: https://doi.org/10.1016/j.envint.2024.109012. Epub 2024 Sep 17. PMID: 39332284.

Wick, R.R., Judd, L.M., Gorrie, C.L., Holt, K.E., 2017. Completing bacterial genome assemblies with multiplex MinION sequencing. Microb. Genom. 3 (10), e000132. https://doi.org/10.1099/mgen.0.000132.

Woh, P.Y., Shiu, H.Y., Fang, J.K., 2024. Microplastics in seafood: navigating the silent health threat and intestinal implications through a one health food safety lens. J. Hazard. Mater. 480, 136350. https://doi.org/10.1016/j.jhazmat.2024.136350.

Zhang, Z., Xu, M., Wang, L., Gu, W., Li, X., Han, Z., Fu, X., Wang, X., Li, X., Su, Z., 2023. Continuous oral exposure to micro- and nanoplastics induced gut microbiota dysbiosis, intestinal barrier and immune dysfunction in adult mice. Environ. Int. 182, 108353. https://doi.org/10.1016/j.envint.2023.108353.

Zhao, S., Liu, R., Lv, S., Zhang, B., Wang, J., Shao, Z., 2024. Polystyrene-degrading bacteria in the gut microbiome of marine benthic polychaetes support enhanced digestion of plastic fragments. Commun. Earth. Environ. 5, 162. https://doi.org/10.1038/s43247-024-01318-6.